

---

## **MORINGA-TiO<sub>2</sub> NANO COMPOSITE (MT2) FOR REMOVAL OF METHYLENE BLUE (MB) AND METHYL ORANGE (MO) DYES FROM THEIR AQUEOUS SOLUTIONS**

---

**G. M. Taha<sup>1</sup> and N. H. Ibrahim<sup>1\*</sup>**

*Environmental Applications of Nanomaterials Lab., Chemistry Department, Faculty of Science,  
<sup>1</sup>Aswan University, Aswan 81528, Egypt.*

\*Corresponding author: [chemist\\_nesma@yahoo.com](mailto:chemist_nesma@yahoo.com)

---

### **ABSTRACT**

Removal and/or degradation of dyes existing in water samples were considered by so many researchers. The present work distinguishes by using a very low cost, highly available and eco- friendly materials as adsorbents. On the other hand, this work considered as unprecedented work where, this is the first time to use moringa seeds as a co-dopant to synthesize the moringa/titania bio-composite. Three different adsorbents (moringa seeds (M2), TiO<sub>2</sub> (T2) and moringa/TiO<sub>2</sub> nano composite (MT2)) were examined for removal of methylene blue (MB) and methyl orange (MO) dyes existing in water samples. Sol-gel method was made use for synthesis both of TiO<sub>2</sub> and the composite. The resulted powders were characterized by scanning electron microscope (SEM) & transmittance electron microscope (TEM) micrographs, EDX, XRD, BET and IR as well. For batch method, the effect of pH, dose, shaking time as well as initial dye concentration were studied. The highest removal for MB was obtained at 10 mg/L where, removal percentages were 39, 61 and 80.5% for T2, M2 and MT2, respectively. On the other hand, the removal percentages of MO were 40.0, 52.5 and 68.4% for T2, M2 and MT2, respectively.

**Keywords:** Moringa, moringa / TiO<sub>2</sub> nanocomposite, dyes, Removal.

### **1. INTRODUCTION**

Water pollution occurs when undesirable effluents disperse in a water stream and hence, water quality adversely affected [1].

Colour is usually the first contaminant to be recognized in a wastewater because a very small amount of synthetic dyes in water (< 1 ppm) are highly visible, affecting the aesthetic merit, transparency and gas solubility of water bodies. They absorb and reflect the sun light entering water, thereby interfering with the aquatic species growth and hindering photosynthesis. Additionally, they can have acute and/ or chronic effects on organisms depending on their concentration and length of exposure [2]. Also, of particular concern are more specific compounds, used throughout the wet-processing steps (one of the dyeing steps), that can be toxic to aquatic life. Those include heavy metals, surfactants (wetting agents), fabric rinsing and/or washing detergents and other additives such as salts, sodium sulphate, sulphuric acid and dispersive agents). Additionally, dyeing baths often use extreme pH values (either acidic or alkaline, depending on the dye) and high temperatures; they have high biological and chemical oxygen demand

(BOD and COD), solids, oil and possibly toxic organics that include phenols [3]. These compounds always change the effluent water, causing a variety of physiological and biochemical disturbance [2].

In the textile industry, up to 200,000 tons of these dyes (10-50%) are lost to effluents every year during the dyeing and finishing operations, due to the inefficiency of the dyeing process [4].

Unfortunately, most of these dyes escape conventional wastewater treatment processes and persist in the environment as a result of their high stability to light, temperature, detergents, chemicals, soap and other parameters such as bleach and perspiration [5].

Coagulation is one of the most common ways to reduce the pollutant contents in the water body that are present as turbidity, color and organic matters. Coagulation is also used to reduce the metal ion content in water. Separation of these colloids can be done by the addition of synthetic coagulant or biocoagulant followed by slow agitation (flocculation) that causes coagulation of colloidal particles so they can be separated by sedimentation [6].

Nanotechnology has been considered effective in solving water problems related to quality and quantity. There are many aspects of nanotechnology to address the multiple problems of water quality in order to ensure the environmental stability [7].

*Moringa oleifera* is the best known species of the *Moringaceae* family. *Moringaceae* is a family of plants belonging to the order *Brassicales*. It is represented by fourteen species and a single genus (*Moringa*), being considered an angiosperm plant. It is fast growing, reaching 12 meters in height. It has an open crown and usually a single trunk. It grows mainly in the semi-arid tropics and subtropics. Since its preferred habitat is dry sandy soil, it tolerates poor soils, such as those in coastal areas [8].

Previous research found that *Moringa* is not toxic [9] and recommended for use as a coagulant in developing countries. It was conducted and showed that moringa seeds are effective as biocoagulant to improve physico-chemical properties of contaminated water.

#### **Titanium Dioxide:-**

The nano-TiO<sub>2</sub> photocatalyst is a well-known photocatalyst among the metal oxides recognized for its high efficiency, low cost, physical and chemical stability, widespread availability and non-corrosive property [10]. TiO<sub>2</sub> exists in three mineral forms: anatase, rutile, and brookite [11].

## **2- EXPERIMENTAL**

### **2-1-Materials:-**

*Moringa oleifera* seeds, and analytical grade of isopropanol, Nano TiO<sub>2</sub> (11.8 nm), methylene blue, methyl orange, HNO<sub>3</sub> (65%) or HCl (37%) and NH<sub>4</sub>OH were used. Deionized water was used for all preparations.

### **2.2 Methods:-**

#### **2.2.1. Pretreatment of Moringa Seeds:-**

After drying moringa seeds at 80°C overnight, the pods were shelled and seeds were ground using agate mortar then the sample was sieved to 64 µm and dried at 80°C overnight once again [12].

#### **2.2.2. Preparation of TiO<sub>2</sub> Nanoparticles:-**

The precursor solution was a mixture of 5 ml titanium isopropoxide, TTIP (97%) and 15 mL isopropanol (99%). A 250 mL of distilled

water with pH 4 was used as the hydrolysis catalyst. The pH value of the solution was adjusted by adding HNO<sub>3</sub> or NH<sub>4</sub>OH (1M). The gel preparation process started when both solutions were mixed together under vigorous stirring. Hydrolysis of TTIP offered a turbid solution which heated up to 60–70°C for almost 18–20 h (peptization). After peptization process, the volume of the solution decreases to 50 mL and a suspension was produced. Depending on the preparation conditions, the resultant suspension was white-blue or opaque with high viscosity.

The prepared precipitates were washed with ethanol and dried for 3 hours at 100°C. After being washed with ethanol and dried at 100°C in a vacuum system for 3 h, a yellow-white powder is obtained. Finally, the prepared powder was annealed at temperature of 600°C for 2 h [13].

#### **2.2.3. Preparation of Moringa-TiO<sub>2</sub> Nanocomposite:-**

Moringa powder (3 g) was allowed to swell in 15 mL of deionized water and stirred for 2 h to get a uniform suspension. At the same time, the TiO<sub>2</sub> (3 g) was dispersed into deionized water (15 mL). Then the diluted TiO<sub>2</sub> was slowly added, drop by drop, into the suspension of moringa and stirring continued for further 5 h. After that, the mixture of 5 mL alcohol and 0.2 mL deionized water was added slowly to the above MT2 mixture and stirring was continued for additional 5 h. The suspension was then kept overnight at room temperature and the obtained precipitate was carefully dehydrated in an oven for 6 h at 80°C [14].

### **2.3. Equipments:-**

The synthesized nanocomposite and the further experiments were characterized all followed by various techniques. X-ray diffraction (XRD) patterns were carried out by using (XRD Brukeraxs D8, Germany) Cu K $\alpha$  radiation 0.154. Surface morphology and elemental analysis of the samples were carried out using Scanning Electron Microscopy with electron dispersion spectroscopy (SEM-EDS) and characterization was conducted using a QUANTAFEG 250, Netherlands. The microscopic nanostructure and particle size were determined using a Transmittance Electron Microscope (TEM), JEOL (JEM-HR-

2100ELECTRON MICROSCOPE, USA). The surface area measurements were made using Burnauer – Emmett- Teller (BET) surface area (Quanta CHROME NOVA2000 Series, UK). The FTIR spectra of samples were recorded through FTIR spectrometer using KBr tablets (JASCO 3600Tokyo, Japan), at room temperature in the range of 400–4000 cm<sup>-1</sup>. The pH measurements were made on digital Adwa AD 1000pH/mV& Temperature Meter, Romania). The absorbance of the samples was measured using Spectrophotometer, (model: UV-1800 TOMOS, China). Centrifuger, SCIOLOGEX (Power Source: 220 VAC, 50 HZ, Speed 45000 rpm, U.S.A.) was used to separate the adsorbent from the mother solution.

#### 2.4. Batch Adsorption Experiment:-

100 ppm stock solutions of MB or MO dyes were prepared by dissolving the appropriate amounts of the dyes in deionized water. The diluted standard solutions of the desired concentrations were daily prepared. 0.5 g of adsorbents (M2, T2 or MT2) was added to 50 mL dye solution. The mixture was shaken for 30, 60, 120, 180, 240 and 360 minute. Mixtures were then centrifuged and the clear solutions were decanted. The free dyes concentrations were determined spectrophotometrically at wavelengths of 664 and 490 nm for MB and MO, respectively. The effect of contact time (30–360 min.), initial dye concentration (10–100 ppm), pH (2–10) and adsorbent dose (0.1–1 g) was studied. The percentage removal (% removal) was calculated using the following equation:

$$\% \text{ Removal} = \frac{C_i - C_f}{C_i} \times 100 \quad (1)$$

Where: C<sub>i</sub> is the initial dye concentration; C<sub>f</sub> is the free dye concentration in solution at equilibrium. Noteworthy, initial and final absorbance of dye solution might used instead.

### 3- RESULTS AND DISCUSSION:-

#### 3.1. XRD Patterns for M2, T2 and MT2:-

The XRD patterns of nanotitania and moringa-TiO<sub>2</sub> nanocomposite are shown in Figure (1).

Moringa exhibits amorphous pattern. It was noticed that, the sample of nanocomposite

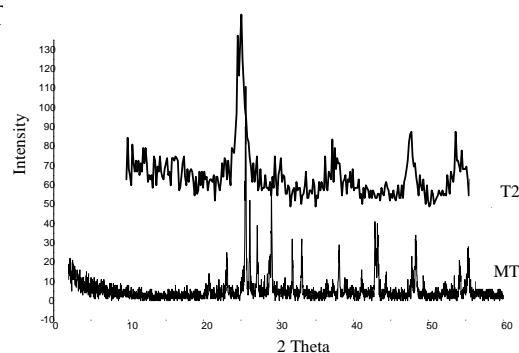


Fig (1) XRD Patterns for (T2) and (MT2)

show two intense peaks at  $2\theta$  of 25.7° and 29.1° and these values reveal to the presence of titania as brookite phase (Paola et al., 2013). The crystallite size was determined by the Scherer's equation [15] and it was found to be 29.8 nm. XRD for the free nano titania in figure (1) indicates that, crystalline mixture of brookite and anatase were obtained at  $2\theta$  of 25.5, 30.6 and 25.3°, respectively and the crystallite size was 11.8 nm.

Due to the high amount of oils and proteins present in the composition of the M2 which represent around 69% of the total mass, it shows unresolved signals (predominantly amorphous) [16].

The data attached with the XRD pattern of MT2 exhibits that Fe, Cu and S are present in SQ% of 5%. In addition Ca, Na, P and Si are representing 12%. All the above mentioned elements were proven (XRF analysis, Table 1) as a mineral content of moringa seeds.

#### 3.2. XRF Analysis:-

Table (1) Chemical Composition of Moringa Seeds

Item	%	Item	%	Item	%
SiO <sub>2</sub>	0.93	MgO	0.75	Cl	0.94
TiO <sub>2</sub>	0.03	CaO	0.65	SO <sub>3</sub>	13.07
Al <sub>2</sub> O <sub>3</sub>	0.24	Na <sub>2</sub> O	0.05	Loss on Ignition	75
Fe <sub>2</sub> O <sub>3</sub>	0.07	K <sub>2</sub> O	3.94		
MnO	0.04	P <sub>2</sub> O <sub>5</sub>	4.08		

The elemental percentages content for the elements existing in the moringa seeds are listed in table (1). The high loss in the mass on ignition may be due to the high organic matters and water content.

#### 3.3. FTIR Analysis for M2, T2 and MT2:-

Chemical composition of moringa shows that, fat has the main component of the moringa seeds and represents 36.7%. Also, the seeds contain protein, carbohydrate, fibre and ash

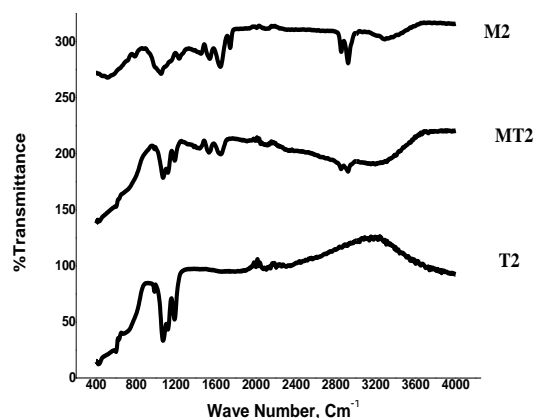


**Fig (3) SEM Micrographs for M2**

which represent 31.4, 8.4, 7.3, and 6.2%, respectively [17, 18].

FTIR for either pure M2, T2 or MT2 nanocomposite are shown in figure (2). This figure shows characteristic band at  $428\text{ cm}^{-1}$  corresponding to Ti-O bond as a weak stretching band [19]. The presence of NH groups chemisorbed on the surface is confirmed by stretching vibration at  $1430\text{ cm}^{-1}$ ,  $2921\text{ cm}^{-1}$  and  $3256\text{ cm}^{-1}$  band. The figure also shows characteristic bands at  $1525$  and  $1642\text{ cm}^{-1}$  corresponding to C=O amide in protein or fatty acids in lipid existing in moringa seeds [20].

### 3.4. Scanning Electron Microscope Micrographs for M2, T2 and MT2:-

SEM graphs indicate that the particles of moringa seeds powder are approximately spherical and bright. Particles have different sizes and the surface appears without any contamination as shown in figure (3). Agglomeration of seeds is obvious [21].

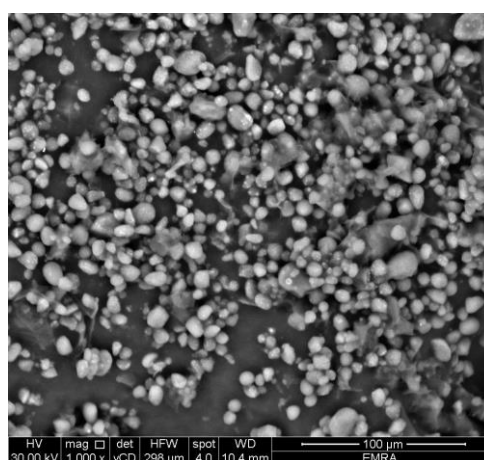
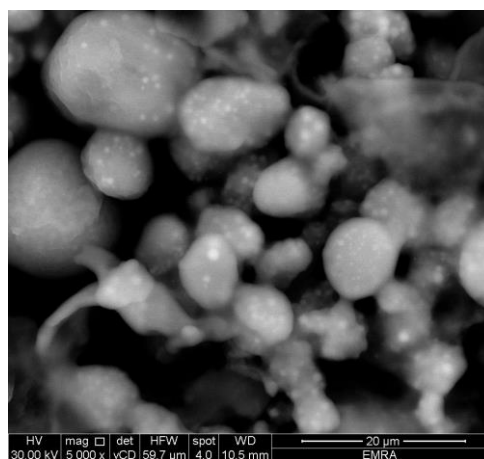
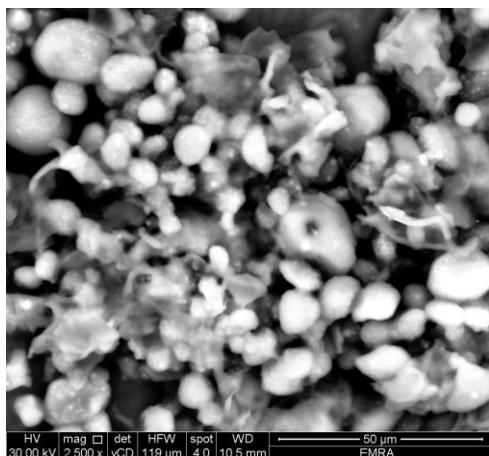


**Fig (3) SEM Micrographs for M2**

The SEM graph for T2 refers to its irregular spherical shape as shown in figure (4). In moringa and titania nano composite, figure (5), the interference between the crystals of T2 and M2 is clear and it has irregular shape due to the disappearance of the characteristic spherical shape of moringa seeds on the formation of the composite.

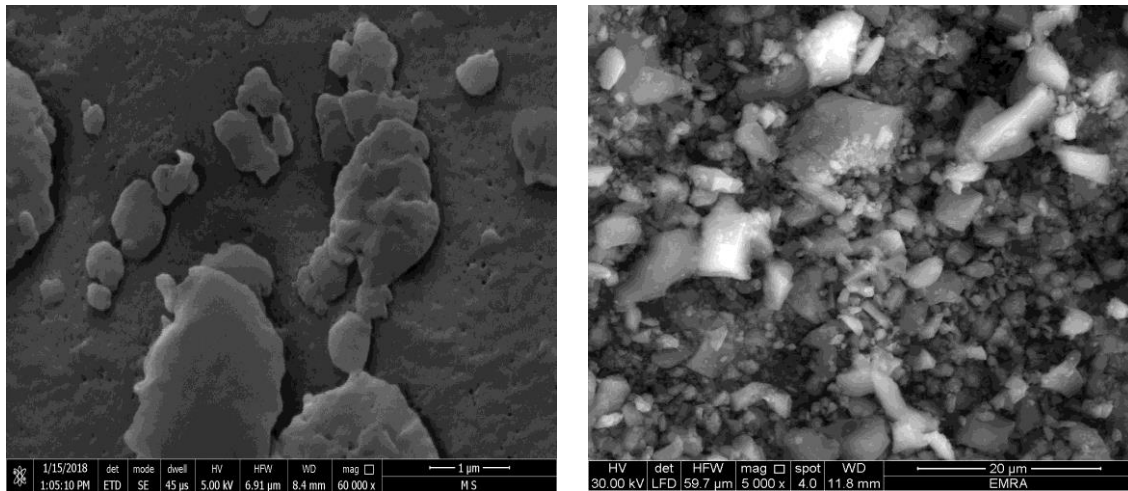


**Fig (4) SEM Micrographs for T2**

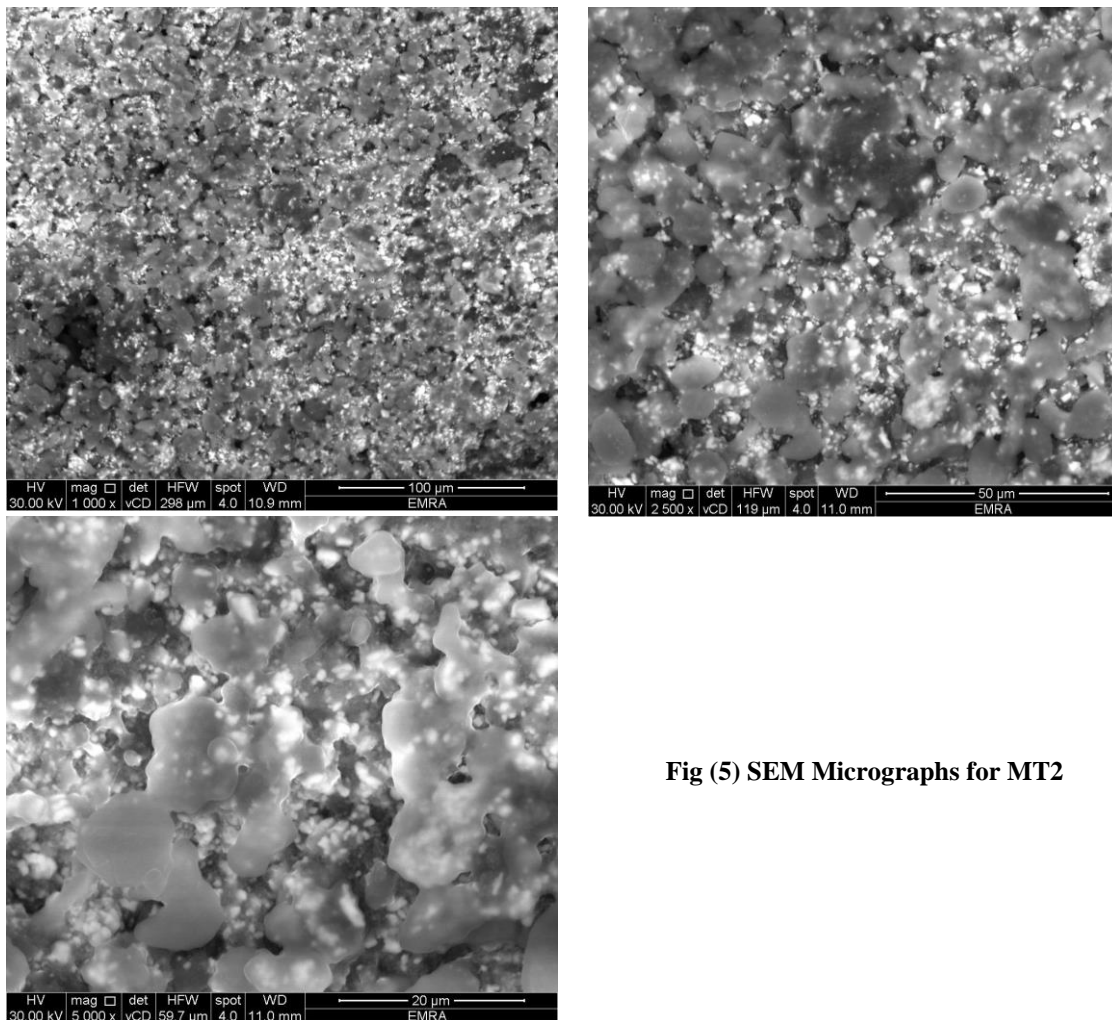


**Fig (5) SEM Micrographs for MT2**

**Table (2) Show the Particle Sizes for M2, T2 and MT2.**

Sample	M2	T2	MT2
Particle size, nm	<b>96.6</b>	<b>14.6</b>	<b>30.8</b>

### 3.5. Transmittance Electron Microscope Micrographs for M2, T2 and MT2:-

No specific crystal structure was shown, Fig 6, in the TEM micrograph of M2 that is due to the amorphous property of M2 (Fig1, XRD pattern).

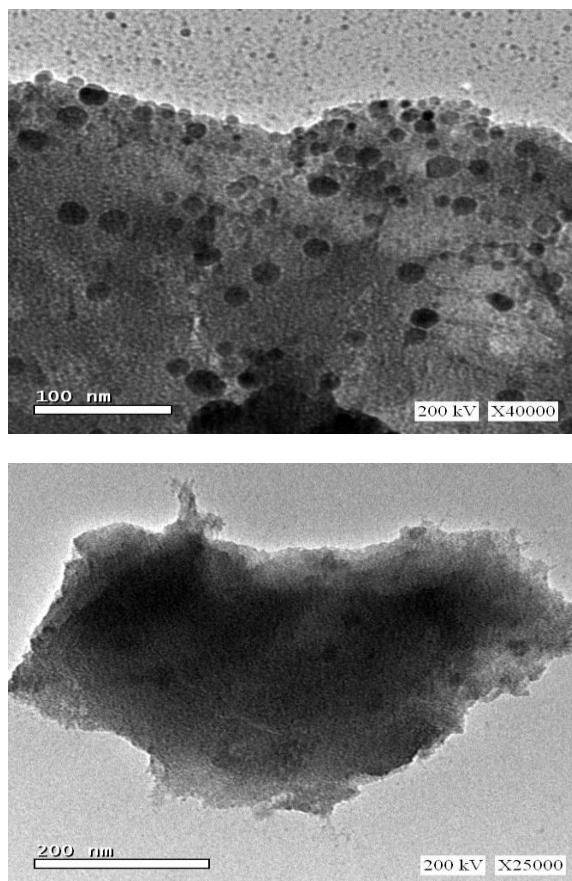


Fig (6) TEM Micrgraphs for M2

It well known that, the different forms of  $\text{TiO}_2$  have different structures thus, tetragonal structure (with dipyramidal habit), tetragonal structure (with prismatic habit) or orthorhombic crystalline structure as shown in figure (7) [22].

In case of MT2 nanocomposite, it gives agglomerated structure including both spherical and orthorhombic as shown in figure (8).

### 3.6. Energy Dispersive X- ray (EDX) for M2, T2 and MT2:-

EDX graphs for the three samples are shown in figures (9-11). The graphs show the specific peaks of Zn, Mg and P before 2keV at energy axis, S and K between 2 – 4 keV and Ti between 4 – 6 keV and 0- 2 keV in pure  $\text{TiO}_2$ . The peaks of Cu and C are related to the instrument. The other peaks are related to the nanocomposite, while the intensity of the peaks is related to the concentration of the element in the imaged spot [23]. These results are confirmed that obtained by XRD (Fe, Cu and S are present in SQ% of 5%. In addition Ca, Na, P and Si are representing 12%) and XRF (Si, Ti, Al, Fe, Mn, Mg, Ca, Na, K, P and S as oxides) with respect to the MT2 nanocomposite.

### 3.7. BET Analysis for M2, T2 and MT2:-

BET analyses for either M2, T2 or MT2 nanocomposite are illustrated in Table (2). Surface area for M2 gives larger value ( $362 \text{ m}^2/\text{g}$ ) than T2 and MT2; which give 57.19 and

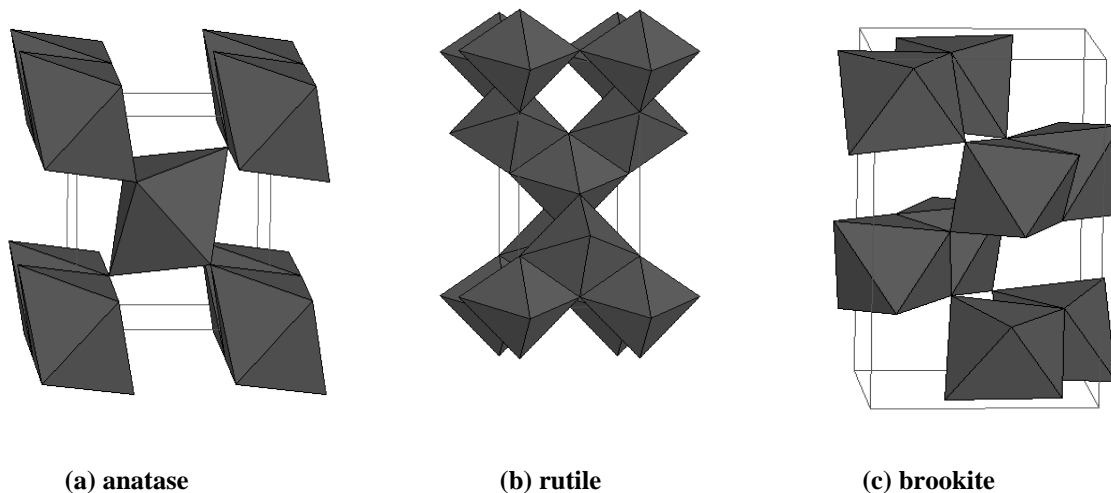
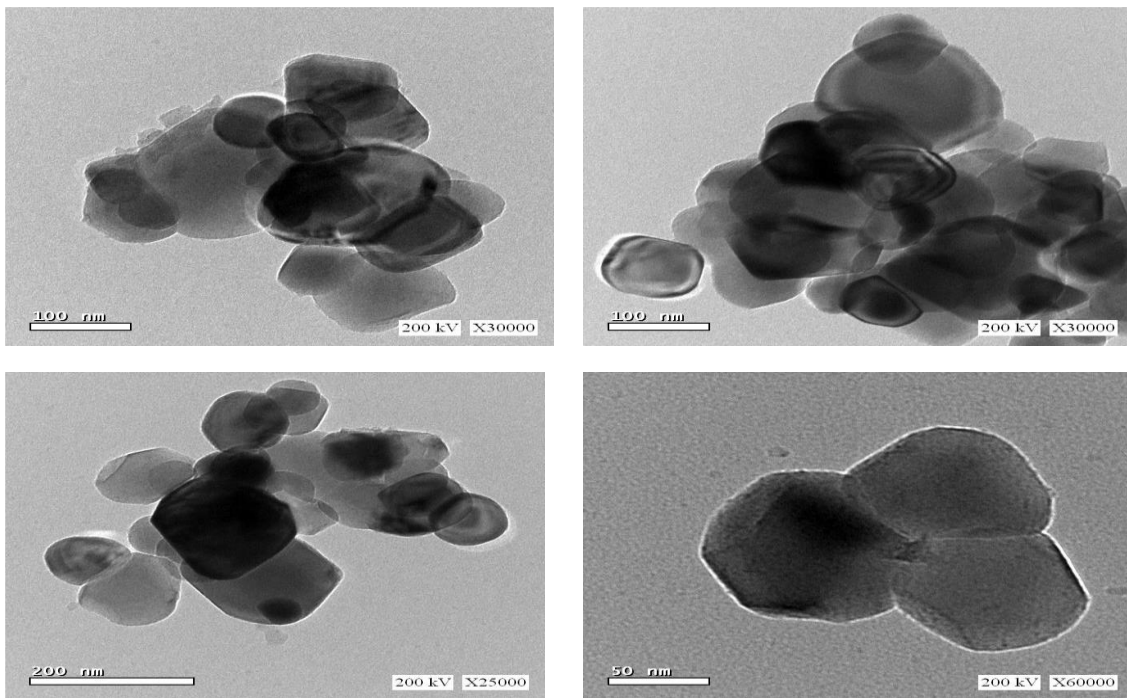


Fig (7) Three Mineral Forms of  $\text{TiO}_2$



**Fig (8) TEM Micrographs for MT2**

C:\SharedData\2017\Fatma\_Ahmed\NH1\NH 1-01.spc

Label A:

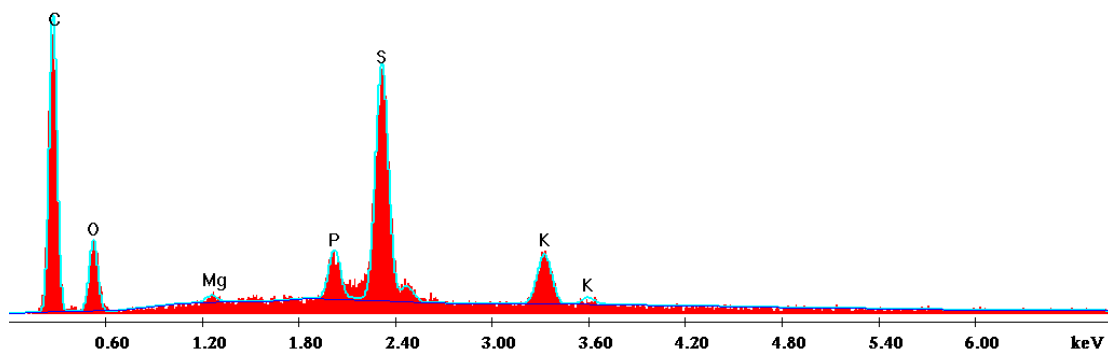


**Fig (9) Energy dispersive X-ray analysis for M2**

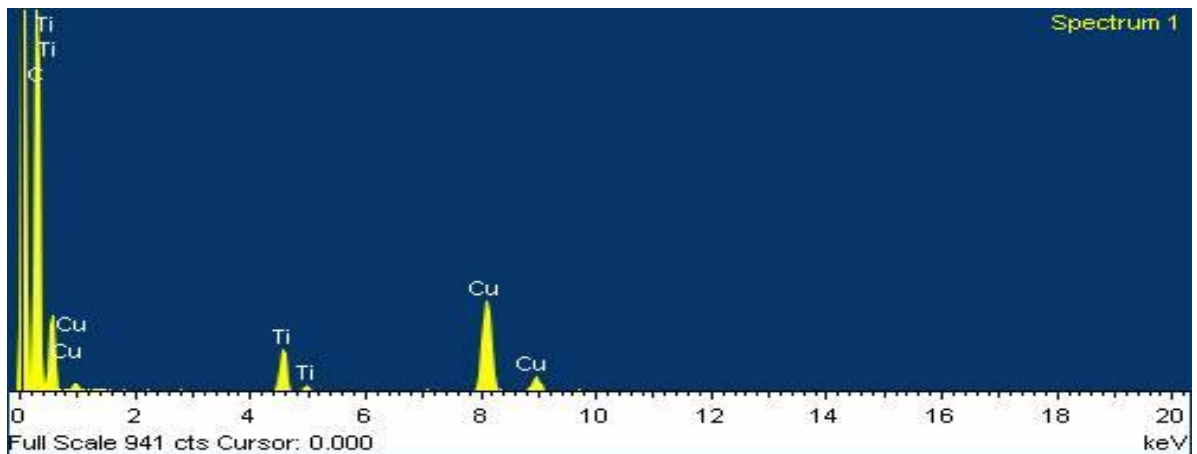


**Fig (10) Energy dispersive X-ray analysis for T2**

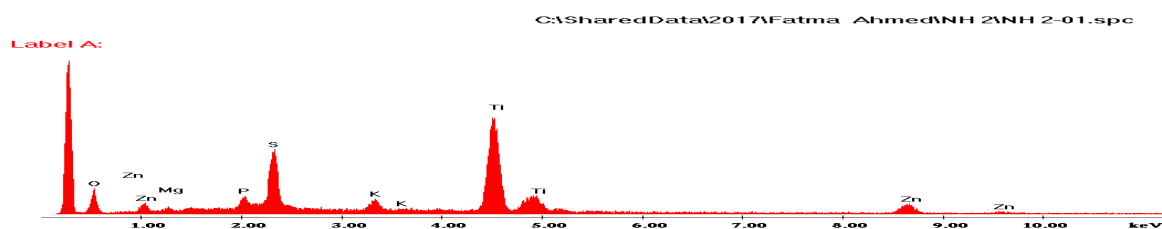


Fig (11) Energy dispersive X-ray analysis for MT2

184 m<sup>2</sup>/g, respectively. [24] reported that the surface area of nano TiO<sub>2</sub> synthesized via sol gel method was 26.274 m<sup>2</sup>/g. [25] reported that, The moringa oleifera seed pod was obtained as a waste from biofloculant. The dried coat was grinded with electrical blender and sieved with 1 mm sieve and the surface area was 2.45m<sup>2</sup>/g.

Table (3) BET Analysis for M2, T2 and MT2

sample	M2	T2	MT2
Surface Area, m <sup>2</sup> /g	362	57.19	184

### 3.8. Effect of pH:-

The adsorption data for the removal of MB and MO on the three adsorbents (M2, T2 or MT2) at various pH values (2 to 10) under the experimental conditions (fixed adsorbent dose, 6 g /L; contact time of 2h; initial concentration of 20 mg/L for each of the dyes) are represented in figures (12&13).

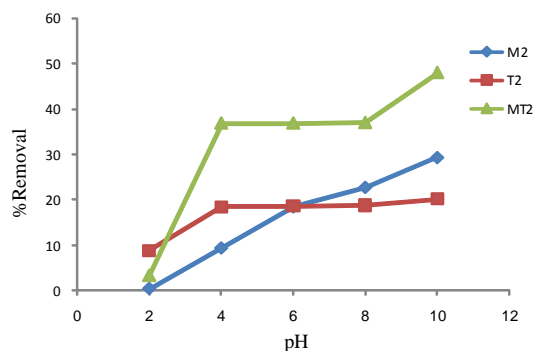


Fig (12) Effect of pH on Methylene Blue Adsorption Using (M2, T2 or MT2).

It is apparent that, the removal percentage of MB by M2 increased with an increase in pH level from 0.45% at pH2 to maximum value of 29.4% at pH 10. The removal percentage of MB by T2 and MT2 increased from pH 2 to 4 and reached to plateau value at pH range of 4 to

8 and then increased at pH 10 to 20.2% and 48% for T2 and MT2, respectively.

The removal percentage of MO by M2, T2 or MT2 increased from pH 2 to pH 6 and then decreased from pH 6 to pH 8 and reached to plateau value at pH range of 8 to 10. The maximum removal percentage of MO was 37, 27.8 and 55.6% at pH 6 by M2, T2 and MT2, respectively.

The basic dye gives positively charged ions when dissolved in water [26]. Thus, in acidic medium the positively charged surface of adsorbent tends to oppose the adsorption of the cationic adsorbate. When pH of dye solution is

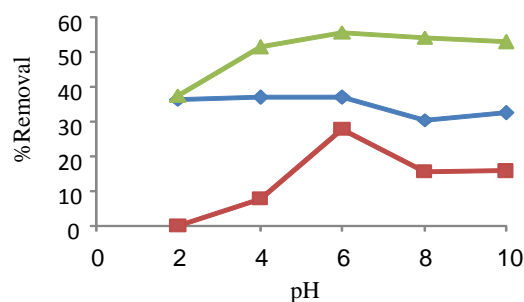


Fig (13) Effect of pH on Methyl Orange Adsorption Using (M2, T2 or MT2).

increased the surface acquires a negative charge, there by resulting in an increased adsorption of MB due to an increase in the electrostatic attraction between positively charged dye and negatively charged adsorbent [27]. The acidic dye gives negatively charged ions when dissolved in water. Thus, in acidic medium the positively charged surface of adsorbent tends to attract the cationic adsorbate. TiO<sub>2</sub> shows an amphoteric character so that either a positive or a negative charge can be developed on its surface and thus a pH variation can influence the adsorption of dye molecules onto the TiO<sub>2</sub> surfaces [28]. Removal of methylene blue by adsorption onto

activated carbon developed from *Ficus carica bast* was observed at pH 8 [29]. The suitable pH for removing MB using moringa seed and NaCl was 8 [30]. The maximum adsorption capacity of the moringa peregrine tree shell ash was at pH 2 for MO removal [31].

### 3.9. Effect of Adsorbent Dose:-

The adsorption data for the removal of MB or MO by the three adsorbents at different dosage 2, 4, 10 or 20 g/L under the same experimental conditions explained in the above mentioned section were studied and represented in figures (14&15).

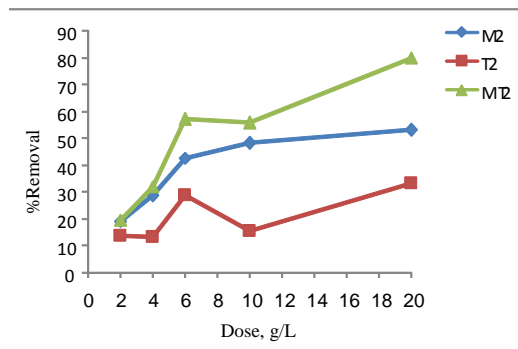


Fig (14) Effect of Dose on Methylene Blue Adsorption

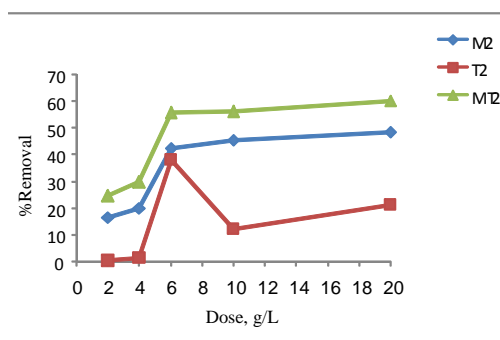


Fig (15) Effect of Dose on Methyl Orange Adsorption

On increasing the adsorbent dose from 2 to 20 g/L, the MB and MO adsorption by the three adsorbents increased. The highest removal for MB was obtained at 20 g/L where, removal percentages were 33.5, 53.5 and 80 % for T2, M2 and MT2, respectively. On the other hand, the removal percentages of MO were 21.1, 59.5 and 69.5% for T2, M2 and MT2, respectively.

It can be concluded that, MT2 is the best adsorbent and it effective toward MB than MO dye. The removal percentage of MO dye at moringa adsorbent dose 1g/L was 69.26% [31]. The optimum dosage using coir pith for MB removal was 40g/L [32]. The optimum dosage using activated carbon developed from *Ficus carica bast* for MB removal was 50 g/L [29].

### 3.10. Effect of Contact Time: -

Removal of MB or MO by the three adsorbents (M2, T2 or MT2) at different contact time (0.5,1, 2, 3, 4 or 6h) under the experimental conditions was studied and results obtained are given in figures (16, 17).

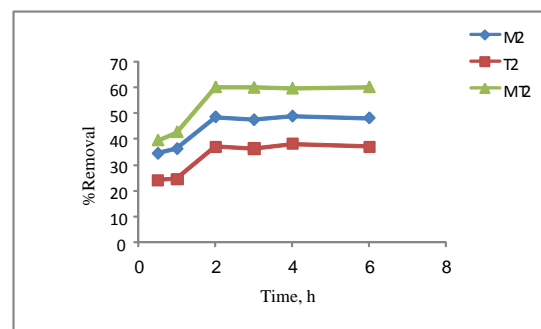


Fig (16) Effect of Contact Time for MB Removal

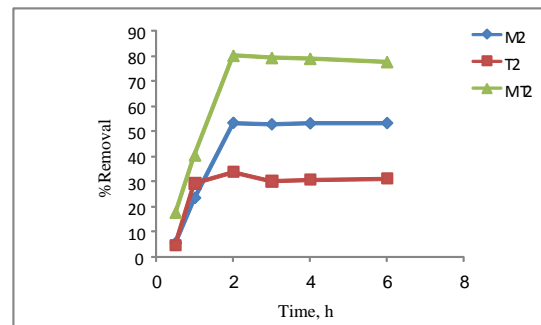


Fig (17) Effect of Contact Time for MO Removal

**Table (4) Removal Percentage of MB and MO for T2**

Concentration, ppm	MB Removal, %	MO Removal, %
10	39.0	40.0
20	37.1	39.0
30	37.0	13.9
50	35.0	8.5
100	14.2	5.0

**Table (5) Removal Percentage of MB and MO for M2.**

Concentration, ppm	MO Removal, %	MB Removal, %
10	61.0	52.5
20	48.4	53.0
30	43.0	54.0
50	27.0	37.0
100	25.0	24.0

**Table (6) Removal Percentage of MB and MO for MT2**

Concentration, ppm	MB Removal, %	MO Removal, %
10	80.5	68.4
20	77.1	60.0
30	64.0	58.0
50	49.0	49.2
100	28.8	27.5

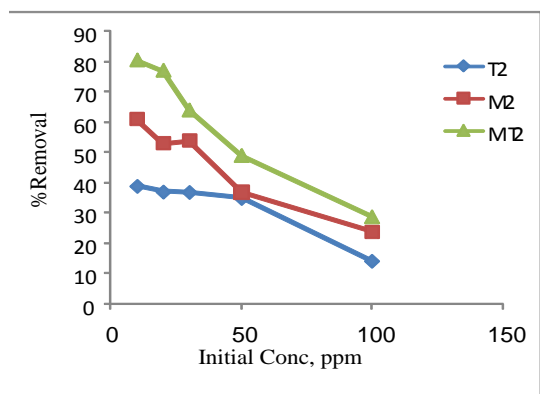


**Fig (18) Effect of Initial Concentration on MB Removal**

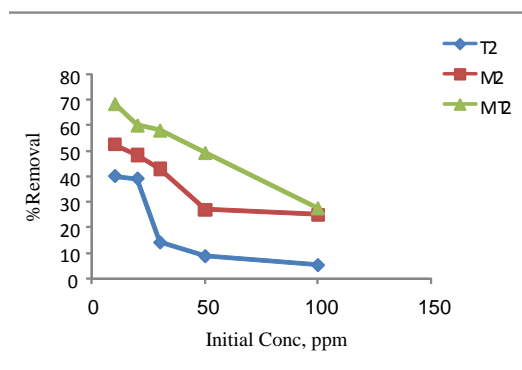


**Fig (19) Effect of Initial Concentration on MO Removal**

The removal percentages below initial concentration (10 ppm) were 100% toward MB or MO dyes. On increasing the initial concentration from 10 to 100 mg/L, the MB and MO adsorption by the three adsorbents decreased. The removal percentages were 39.0, 61.0 and 80.5% for T2, M2 and MT2, respectively. On the other hand, the removal percentages of MO were 40.0, 52.5 and 68.4% for T2, M2 and MT2, respectively. It can be concluded that, MT2 is the best adsorbent and it effective toward MB than MO dye. The maximum concentration using activated carbon developed from *Ficus carica bast* for MB removal was 500 ppm [29].

**4. CONCLUSION:-**

Nanocomposite of titania and moringa was prepared using the same ratio of titania and moringa seeds powder. The XRD results revealed that, the samples prepared in nano size. FTIR and XRF analysis for moringa compatible with XRD results and this confirm the composite formation. Adsorption of MB or MO dyes by the three samples (M2, T2 or MT2) was investigated. Various parameters such as (pH values, adsorbent dose, contact time and initial dye concentration) were tested. The results show that, MT2 nanocomposite gives the best removal for MB (80.5%) or MO (68.4%) dyes at pH 10 and 6 respectively. The best removal can be observed at adsorbent dose 20 g/L, 2 hour and initial concentration 10 ppm for the two dyes.

## REFERENCE

- [1] Alrumman, S. A. and El-Kott, A. (2013). "Water Pollution: Source and Treatment." *American Journal of Environmental Engineering*, V. 6(3), pp. 88-98.
- [2] Pereira, L. R.; Alves, M. S. (2012). "Dyes-Environmental Impact and Remediation.", chapter 4, pp. 111-161. A. Malik, E. Grohmann (eds.), Springer Science+Business Media B.V.
- [3] Shrestha, S. and Kazama, F. (2007). "Assessment of surface water quality using multivariate statistical techniques: a case study of the Fuji river basin, Japan." *Environ Model Software*, V. 22, pp. 464-475.
- [4] Hema, N. and Suresha, S. (2015), "Optimization of culture conditions for decolorization of Acid Red 10B by *Shewanella putrefaciens*." *Int.J.Curr.Microbiol.App.Sci*, V. 4(5), pp. 675-686.
- [5] Couto, S. R. (2009). "Dye removal by immobilised fungi." *Biotechnology Advances*, V. 27(3), pp. 227-235.
- [6] Tebbut, T. H. (1982), "Principles of Water Quality Control." Translate edition, Mohajit. Bandung: ITB. Indonesia.
- [7] Samanta, H. S.; Das, R. and Bhattachajee, C. (2016), "Influence of Nanoparticles for Wastewater Treatment- A Short Review." *Austin Chem Eng.*, V. 3(3), pp. 1036.
- [8] Chaudhary, K. and Chaurasia, S. (2017), "Neutraaceutical properties of moringa oliefera: a review." *Europen Journal of pharmaceutical and medical research*, V. 4(4), pp. 646-656.
- [9] Grabow, W. O.; Slabert, J. L.; Morgan, W. S. and Jahn, S. A. (1985), "Toxicity and Mutagenicity Evaluation of Water Coagulated with Moringa oleifera Seed Preparations Using Fish, Protozoan, Bacterial, Enzyme, and Ames Salmonella Assays." *Water SA*, V. 11, pp. 9.
- [10] Serpone, N. (2018), "Heterogeneous Photocatalysis and Prospects of TiO<sub>2</sub>-Based Photocatalytic DeNO<sub>x</sub>ing the Atmospheric Environment." *Catalysts*, V. 8, pp.1-98.
- [11] Puma, G. L.; Bono, A.; Krishnaiah, D. ; Collin, J.G. ; Haz, J. and Mat. (2008). "Preparation of titanium dioxide photocatalyst loaded onto activated carbon support using chemical vapor deposition." *hazardous materials*. V. 157, pp. 209–219.
- [12] Ravikumar, K. and Sheeja, A. K. (2013). "Heavy Metal Removal from Water using Moringa oleifera Seed Coagulant and Double Filtration." *International Journal of Scientific and Engineering Research*, V. 4, pp. 10-13.
- [13] Mahshid, S.; Askari, M. and Ghamsari, M. S. (2007), "Synthesis of TiO<sub>2</sub> Nanoparticles by Hydrolysis and Peptization of Titanium Isopropoxide Solution", *Journal of Materials Processing Technology*, V. 189, pp. 296–300.
- [14] Mohanapriya, T. and Kumar, P. E. (2015). "Kinetics and Equilibrium Study on the Removal of Ni (II) Using Activated Carbon-Tio<sub>2</sub> Nano Composite." *International Journal of Science and Research (IJSR)*, V. 4, pp. 1439-1445.
- [15] Scherrer, P. (1918), "Bestimmung der Grösse und der inneren Struktur von Kolloidteilchen mittels Röntgenstrahlen." *Nachr. Ges. Wiss. Göttingen*, V. 26, pp. 98-100.
- [16] Araújo, C. S.; Melo, E. I.; Alves, V. N. and Coelho, N. M. (2012), "Moringa oleifera Lam. seeds as a natural solid adsorbent for removal of Ag<sup>I</sup> in aqueous solutions." *Journal of the Brazilian Chemical Society*, V. 21(17), pp. 21-32.
- [17] Anwar, F.; Ashraf, M.; Bhangar, M. I. (2005), "Interprovenance variation in the composition of Moringa oleifera oilseeds from pakistan." *J. Am. Oil Chem. Soc.*, V. 82, pp. 45–51.
- [18] Rahman, I. M. M.; Barua, S.; Nazimuddin, M.; Begum, Z.A.; Rahman, M.A.; Hasegawa, H. (2009), "Physicochemical properties of Moringa oleifera Lam. Seed oil of the indigenous cultivar of bangladesh." *J. Food Lipids*, V. 16, pp. 540–553.
- [19] Van der Marel, H. W. and Beutelspacher, H. (1976), "(Herausg.): Atlas of infrared spectroscopy of clay minerals and their admixtures." Elsevier, Amsterdam 1976. VIII + 396 Seiten, Großformat Dfl. 165, V. 140, issue. 2, pp. 247-248.
- [20] Reddy, D. H.; Seshaiaha, K.; Reddyb, A. V. and Leec, S. M. (2012). "Optimization of Cd(II), Cu(II) and Ni(II) biosorption by chemically modified Moringa oleifera leaves powder." *Carbohydrate Polymers*, V. 88, pp. 1077–86.
- [21] Kumari, P.; Sharma, P.; Srivastava, S. and Srivastava, M. M. (2006). "Bio sorption studies on shelled Moringa oleifera Lamarck seed powder: Removal and recovery of arsenic from aqueous system." *Int. J. Miner. Preece*, V. 132 (78), pp. 131–139.
- [22] Meacock, G.; Taylor, K. D.; Knowles, M. G. and Himonides, A. (1997), "The Improved Whitening of Minced Cod Flesh Using Dispersed Titanium Dioxide", *J. Sci. Food. Agric.*, V. 73, pp. 221-225.
- [23] Bello, O. S.; Adegoke, K. A.; Akinyunni, O. A. (2015), "Preparation and characterization of a novel adsorbent from Moringa oleifera leaf." *Appl Water Sci*, V. 7, pp. 1295–1305.
- [24] Singh, I. and Birajdar, B. (2017), "Synthesis, characterization and photocatalytic activity of mesoporous Na-doped TiO<sub>2</sub> nanopowder prepared via a solvent-controlled nonaqueous sol-gel route." *RSC Adv.*, V. 7, pp. 54053–54062.

## المخلص العربي:

- [25] Abdullah, N. S.; Hussin, M. H.; Sharifuddin, S.S. and Azroie, M. (2017), "Preparation and characterization of activated carbon from moringa oleifera seed pod." *Sci.Int. (Lahore)*, V. 29(1), pp. 7-11.
- [26] Boumediene, M.; Benaïssa, H.; George, B.; Molina, S. and Merlin, A. (2018), "Effects of pH and ionic strength on methylene blue removal from synthetic aqueous solutions by sorption onto orange peel and desorption study." *J. Mater. Environ. Sci.*, V. 9(6), pp. 1700-1711.
- [27] Abd, E. L.; Latif, M. M. and Ibrahim, A. M. (2009). "Adsorption, kinetic and equilibrium studies on removal of basic dye from aqueous solutions using hydrolyzed oak sawdust." *Desalin. Water Treat.*, V. 6, pp. 252-268.
- [28] Wang, N.; Li, J.; Zhu, L.; Dong, Y.; Tang, H. (2008), "Highly photocatalytic activity of metallic hydroxide/titanium dioxide nanoparticles prepared via a modified wet precipitation process." *J Photochem Photobiol A*, V. 198, pp. 282-287.
- [29] Pathania, M., De Jay, N., Maestro, N., Harutyunyan, A. S., Nitarska, J., Pahlavan, P., Henderson, S., Mikael, L. G., Richard-Londt, A. and Zhang, Y., 2017, "Cancer Cell ", V. 32, pp. 684-700
- [30] Mahalakshmi, M. and Saranaathan S. E. (2017), *Moringa oleifera*: A cost effective coagulant for dye degradation, *Rasayan J. Chem.*, V. 10(4), pp. 1097-1103.
- [31] Bazrafshan, E.; Zarei, A. A.; Nadi, H. and Zazouli, M. A. (2014), "adsorptive removal of methyl orange and reactive red 198 dyes by moringa peregrine ash." *Indian journal of Chemical Technology*, V. 21, pp. 105-113.
- [32] Jeyanthi and Masilamai, D. (2012), "Study of the removal of methylene blue from aqueous solution by using coir pith." *Journal of Experimental Sciences*, V. 3(9), pp. 21-26.

تمت دراسة إزالة و / أو التفسخ الحفزي للصبغات الموجودة في عينات المياه من قبل العديد من الباحثين. يتميز هذا العمل باستخدام مواد منخفضة التكلفة للغاية، متوفرة وصديقة للبيئة كمادة مازة. من ناحية أخرى، يُعتبر هذا العمل غير مسبوق، حيث أنه هذه هي المرة الأولى التي تُستخدم فيها بذور المورينجا في تحضير متراكب نانومتري مع التيتانيا. تم استخدام ثلاثة من المواد المازة وهي بذور المورينجا (M2)، التيتانيا (T2) ومتراكب المورينجا مع التيتانيا (MT2). تم استخدام طريقة السول-جيل في تحضير كل من التيتانيا والمتراكب MT2. تم توصيف العينات السابقة باستخدام أشعة الحبود السينية، المجهر الإلكتروني الماسح، المجهر الإلكتروني النافذ، مطياف تحويل فورييه بالأشعة تحت الحمراء، الطاقة المشتتة للأشعة السينية كما تم تقدير أسطح العينات المحضرة. تم دراسة تأثير الرقم الهيدروجيني، جرعة العينة، زمن الإهتزاز وكذا التركيز الابتدائي لكل صبغة.

تم الحصول علي أعلى إزالة لصبغة الميثيلين الأزرق عند تركيز 10مجم/لتر، وكانت نسب الإزالة كما يلي: 39.0، 61.0 و 80.5% علي سطح كل من التيتانيا، المورينجا ومتراكب المورينجا والتيتانيا، علي التوالي. علي الجانب الآخر، كانت نسب الإزالة لصبغة الميثيل البرتقالي كالتالي: 40.0، 52.5 و 68.4% علي سطح كل من التيتانيا، المورينجا و متراكب المورينجا مع التيتانيا، علي التوالي.